

The Interface Behavior Analysis of Thin Film during Ball Indentation Testing

Avelino Manuel da Silva Dias*, Everton Carneiro da Silva

Department of Mechanical Engineering (DEM), Federal University of Rio Grande do Norte (UFRN), Natal, Brazil

Abstract The search for improved tribology properties in materials contributes to the development of processes that extend the useful life of components and their applications in increasingly severe environments. In this respect, thin ceramic films have been used to enhance the properties of components that operate under these conditions. However, expensive experimental assays are needed to assess the behavior of these films and system compounds by films and substrates. These experimental analyses are also destructive, requiring the use of sophisticated equipment and specialized hand tools. On the other hand, with advances in computational mechanics, the application of numerical analysis to solve numerous technological problems has become increasingly common, owing to its low operational costs. This study aims to simulate indentation testing with a spherical penetrator in systems composed of thin CrAlN ceramic film deposited on AISI 4140 metallic substrate using a Finite Element commercial code. The main objective of this study was to evaluate the field behavior of stresses in the contact region of the indenter with the sample and on the film-substrate interface.

Keywords Finite Element, Ball Indentation Testing, Thin Film, Interface Behavior

1. Introduction

The need to improve mechanical properties, such as resistance to oxidation and wear, has led to advances in surface engineering. This field of engineering involves the preparation and modification of surfaces to fulfil specific functions within certain applications. One of the options employed to improve these surface properties is the use of ceramic coatings obtained by deposition processes such as Physical Vapour Deposition (*PVD*). However, the mechanical properties of these films and their interface as substrate must be assessed.

Indentation tests have been applied during the last hundred years to determine surface hardness in different classes of materials. In recent years, instrumented indentation testing has been used to characterize tribology systems [1]. The instrumented indentation technique is conducted using precision instruments equipped with sensors that monitor variations in penetration depth (h) of a penetrator as a function of the applied load (P) when it penetrates the study material, reaches maximum displacement, and then returns to the initial position, completing a loading and unloading cycle [2]. Due to their versatility, a large number of studies have been carried out to investigate new methodology and applications for these

assays. Recent proposals used indentation tests as a tool to assess the mechanical characteristics of materials such as surface hardness (H), Young's modulus (E), Poisson coefficient (ν), fracture toughness (K_{IC}), film thickness (t) and a stress behavior curve as a function of elastic-plastic strain [3-9]. However, implementation of this experimental methodology to assess mechanical properties and the results obtained still raise doubts in the scientific community. According to the literature, these problems are more serious when assessing the mechanical behavior of thin films deposited on soft substrates [2, 7].

Due to these limitations in analysing indentation tests, the use of a numerical technique capable of evaluating stresses and strains during the indentation cycle may contribute to a better interpretation of this test. Recently, this numerical methodology has been studied using the Finite Element Method (*FEM*) to assess the behavior of different materials in indentation testing [9-15].

The *FEM* has been proved a reliable numerical technique for analysing stresses and strains and simulating different engineering problems. This method has widely been used to simulate and resolve numerous nonlinear problems related to structural instability and dynamic, electromagnetic, and mechanical forging process. However, the use of this numerical technique to assess the indentation test in thin surface coatings has also had problems mainly due to computational limitations, difficulty in implementing damage criteria and, chiefly, in characterizing these coatings [7, 14-16].

The simulation presented in this study used *FEM* models

* Corresponding author:

avelino.dias@ct.ufrn.br (Avelino Manuel da Silva Dias)

Published online at <http://journal.sapub.org/ijme>

Copyright © 2016 Scientific & Academic Publishing. All Rights Reserved

to reproduce the indentation test with a spherical indenter, as illustrated in Fig. 1. The system under study was composed of a metallic substrate coated with different thicknesses of a ceramic film. A simulation was also used to assess the mechanical behavior of the interface in these systems that combine high-hardness coatings with a middle-hardness substrate. This interface was modelled by introducing a thin layer of elements with mechanical properties capable of simulations ranging from perfect adhesion to possible delaminating of the film.

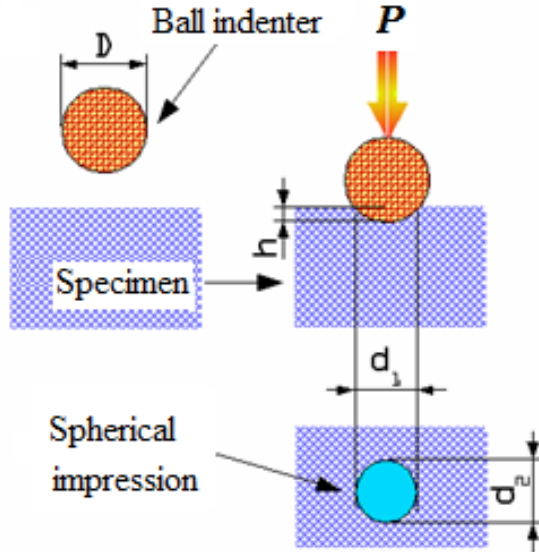


Figure 1. Illustration of ball indentation testing, where D is the diameter of the indenter, h is the indentation depth, d_1 and d_2 are diameters of the impression at specimen and P is the force applied to the indenter [1]

2. Methodology

The numerical simulation performed in the present study used the finite element commercial software to model the indentation test with a spherical penetrator in a thin ceramic film deposited on a metallic substrate [17]. Due to the symmetry of the problem, axis symmetric elements were used in the numerical model, significantly decreasing computational efforts [1]. The studied system was composed of an AISI 4140 alloy steel substrate coated with a chromium aluminium nitride (CrAlN) film with four different thicknesses, i.e., 1.67 μm , 3.00 μm , 6.00 μm and 9.00 μm . These studied materials, of both the film and the substrate, were considered isotropic and homogeneous. The elastic-plastic behavior of these materials was illustrated by means of a curve depicting the linear elastic regime and plastic yield (Equation 1), primarily as described by Hosford and Caddell [18]. In this expression, σ and ε are effective stress and yield limit, respectively. K is a constant that describe the strain hardening characteristics of the material and n known as the strain-hardening coefficient [7-8, 18].

$$\sigma = \begin{cases} K\varepsilon^{1.0} \\ K\varepsilon^n \end{cases} \quad (1)$$

Table 1 shows the mechanical properties of the film and the substrate adopted in the present study. The experimental values of Young's modulus (E), yield limit (σ_o) and Poisson coefficient (ν), as well as Equation (1) data, were obtained from the literature [15, 19].

In an attempt to simulate interface behavior during the simulations, a layer with the lowest thickness possible was introduced between the film and the substrate (Fig. 2). This layer was modelled with a thickness of 0.0834 μm using one ply of elements or with a thickness of 0.167 μm using two-ply. In addition, the interface behavior was modelled as perfectly plastic in order to allow slip between the film and substrate. The yield strength (σ_o) adopted for this layer was the same as the substrate. To complete its behavior model, its Young's modulus (E) was varied between 238.00 GPa and 1.00 GPa. The first value was equal to the Young's modulus of the substrate, which represented perfect adhesion. The latter value represented weak adhesion between the film and the substrate. The characteristics of the meshes used in the different numerical models were listed in Table 2.

Table 1. Mechanical properties adopted for the film and substrate [15, 19]

	Substrate (AISI 4140 steel)	Film (CrAlN)
E (GPa)	238.00	350.00
ν	0.29	0.22
σ_o (MPa)	565.00	3,790.00
K (MPa)	2,230.00	10,615.00
n	0.228	0.299

Table 2. Characteristics of the meshes used in numerical models simulated with a system composed by film, interface and substrate

Film CrAlN with AISI 4140 alloy steel substrate		
Substrate	8,550 elements	
Film	1.67 μm thickness	525 elements
	3.00 μm thickness	945 elements
	6.00 μm thickness	1,890 elements
	9.00 μm thickness	2,835 elements
Interface	One ply	105 elements
	Two-ply	210 elements

The indentation cycle (loading and unloading phases) was simulated using the prescribed displacement of the penetrator, allowing better numerical control at the outset and during simulation of the test [13, 15]. The incremental analysis of the problem used one hundred increments for both the loading and the unloading phases. The numerical model used four-node isoparametric axis-symmetric elements. In order to obtain better distribution of the field of stresses and strains in the contact region of the indenter and at the interface with the substrate, a more refined grid was utilized in these regions, Fig. 2. The decrease in element size increases the rising computational costs, but reduces instability in the numerical result of the loading curve as a function of displacement in these simulations [1].



Figure 2. Numerical model at the contact region of ball indentation testing in a system with film, interface and substrate

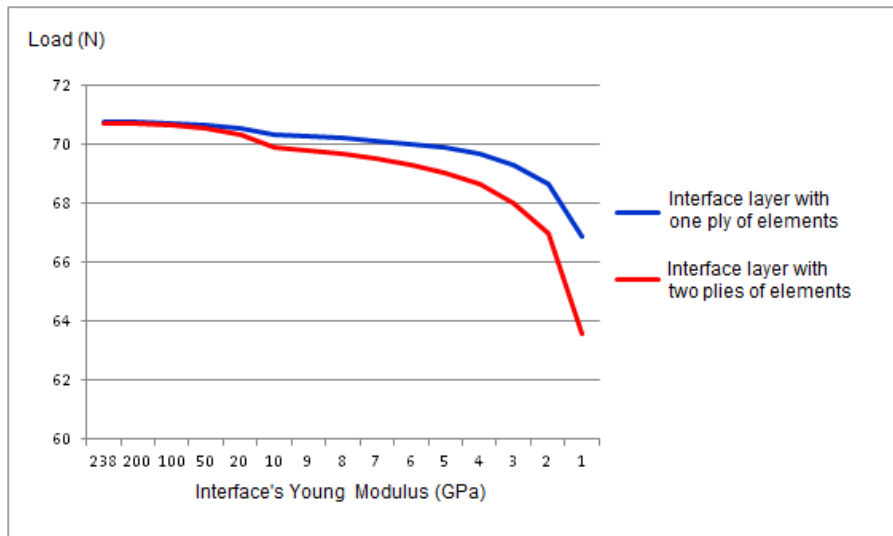


Figure 3. Behavior of the maximum indentation load as a function of Young's modulus at the interface for the system with 3.00 μm thick film

Indenter penetration depths of 10%, 20%, and 50% of film thickness were adopted. According to the literature, a penetration depth of up to 10% of film thickness was used when studying film without the influence of the substrate [10, 16]. Other authors recommend that this thickness be up to 20% when the substrate exhibits high mechanical strength [7]. To assess the behavior between the film and substrate system, the present study adopted a depth of half the film thickness. A friction coefficient between the indenter and surface of the film was not considered, because this friction has no significant influence on indentation load [20]. Also, the pile-up and sinking-in surface displacements, which could occur during the indentation testing, were not taken into account in the present analysis [7, 13, 15].

3. Results and Discussions

Table 3 illustrates numerical results of the maximum

indentation load as a function of Young's modulus in the interface for a model with two different thick film and a penetration depth at a half of these thicknesses. It was considered to be optimal adhesion between film and substrate when the interface modulus was equal with the substrate, i.e., 238 GPa. The value of Young's modulus was reduced gradually, where indentation testing with low adherence between the film and the substrate was simulated. The numerical results for indentation load show little change in its value in the function of the variation of the interface modulus and the number of ply of the interface. However, in all cases, for low values of the modulus of elasticity, for example, less than 10.0 GPa for 1.67 μm thick film, there is a significant reduction of indenter load, in both of the different models used to represent the interface. However, for thicker films, this behavior was less critical. In other words, a greater film thickness leads to a better distribution of the stresses in the film, without overloading the interface. This behavior of thicker films has been observed in the literature [1, 3].

Table 3. Maximum indentation load as a function of Young’s modulus at the interface for two different systems

Young modulus at the interface	Indenter load (N)			
	1.67 μm thick film		6.00 μm thick film	
	One ply	Two-ply	One ply	Two-ply
238 (GPa)	46.16	46.14	110.00	110.00
200 (GPa)	46.16	46.13	110.00	109.90
100 (GPa)	46.13	46.08	110.00	109.90
50 (GPa)	46.07	45.96	109.90	109.90
20 (GPa)	45.90	45.65	109.80	109.70
10 (GPa)	45.64	45.14	109.70	109.30
8 (GPa)	45.51	44.90	109.60	109.20
6 (GPa)	45.29	44.52	109.50	108.90
4 (GPa)	44.89	43.77	109.20	108.50
2 (GPa)	43.77	41.74	108.50	107.10
1 (GPa)	41.89	38.59	107.10	104.60

The reduction in indentation load value shown in Fig. 3 illustrates the possibility of simulation of delamination of the film during the indentation testing, when reducing the value of Young’s modulus at interface. Another important result in these analyses was that the decrease in the indentation load was more pronounced when using two-ply of elements in the interface.

At the end of this work, a comparison was made between the relative radial displacement of two neighbouring nodes positioned at the interface and with the same distance from the axis of symmetry. Fig. 4 shows the behaviour of the radial displacement of those two nodes (nodes 103 and 8,634)

for the model on which the interface was modelled with a layer of 0.167 μm and with Young’s modulus of 200 GPa. Fig. 5 shows the same situation, but with Young’s modulus at the interface equal 2.0 GPa. It could verify that for the lower Young’s Modulus at the interface there are higher relative displacements for these neighbouring nodes identified previously. This slip indicates the occurrence of delamination process on interface. These results are similar with the one shown by Araújo and Dias (2014), but in the present analysis, the interface was modelled with two-ply of elements.

Finally, for all simulations models, there was a decrease of the maximum indentation load by reducing the value of the Young’s modulus at the interface. There were also higher interface slip behaviors because of decrease of the Young’s modulus. In opposite, it was shown that for the simulated models with higher values of Young’s modulus at the interface, the radial displacement behavior of the nodes in question is quite similar in all systems studied. This result indicates that the interface model ensured adhesion between the film and the substrate, i.e., no delamination occurred.

Other studies found in the literature showed how to model the interface through decohesives elements [14, 18]. However, to better simulate the behaviour of the interface, these models require that know the fracture toughness of the film or of the interface [14]. These mechanical properties require destructive experimental testing, expensive cost and time consuming. The numerical model proposed here has the advantage of avoiding adding further mechanical properties simulation than those described in Table 1.

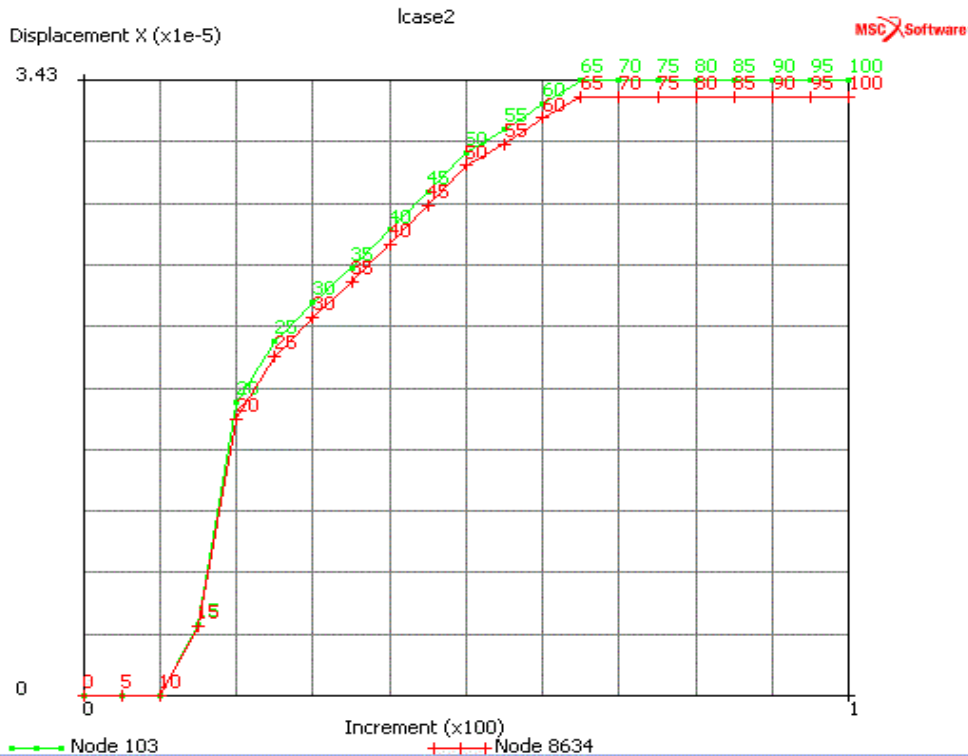


Figure 4. Graph of radial displacement between node 103 and node 8,634 during indentation testing for a system with 3.00 μm thick film and two-ply of elements at interface, with Young’s modulus of 200 GPa

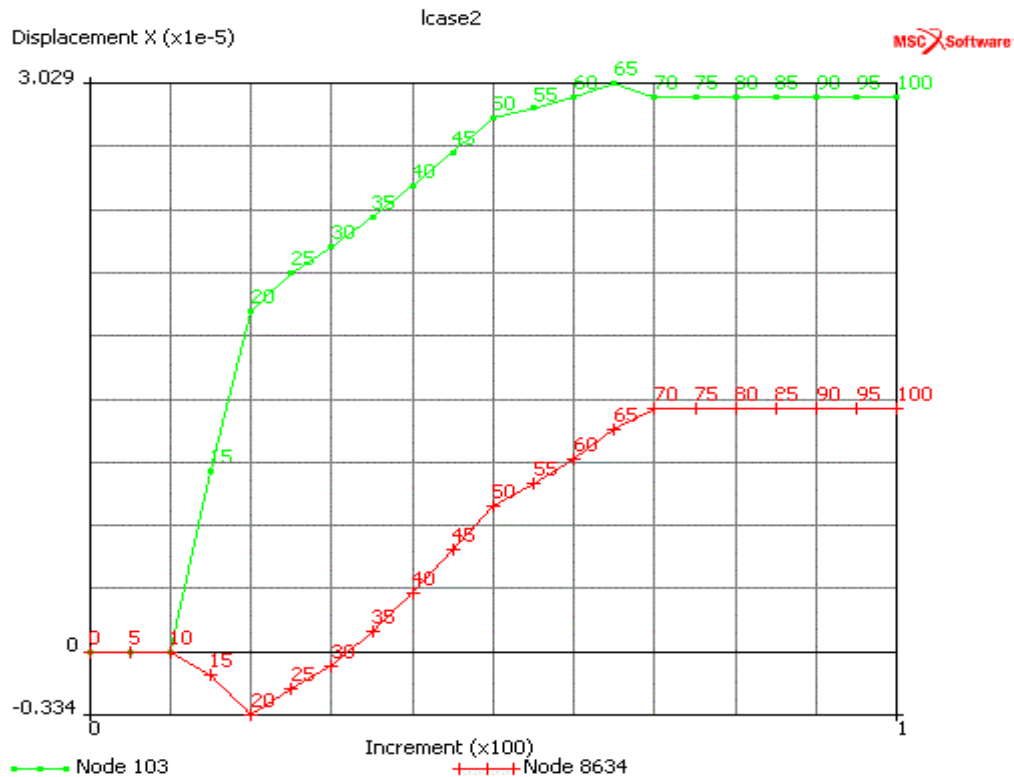


Figure 5. Graph of radial displacement between nodes 103 and 8,634 during indentation testing for a system with 3.00 μm thick film and two-ply of elements at interface, with Young's modulus of 2.0 Gpa

4. Conclusions

Based on the numerical results of the indentation test with spherical indenters using the finite element method, it was concluded that from its overall behavior, the models represent the indentation test in different systems composed of a hard film (CrAlN), with different thicknesses, deposited in a metallic substrate with high mechanical strength (AISI 4140 steel).

In this study, an attempt to represent the behavior of the interface region during the indentation testing by varying the refinement of the mesh, the value of its Young's modulus and the number of ply elements. The results showed that the models were able to represent since a perfect adhesion between the film and the substrate to a weaker adhesion. Evaluating these results, by analyse the maximum load indentation was possible to identify delamination of interface region for the lowest values of its Young's modulus.

However, there is still need for a more thorough numerical and experimental analysis in order to introduce a parameter capable of more representative modelling of film-substrate adhesion.

ACKNOWLEDGEMENTS

The authors gratefully acknowledge the financial support by CNPq (Brazilian foundation for the support of research), under grants process 460943/2014-6 MCTI/CNPq/Universal

2014. They also thanks for the CAPES (Higher Coordination Brazilian Agency for Scientific and Educational Training), through process BEX 6569-14.

REFERENCES

- [1] Araújo, R., and Dias, A.M.S., 2014, Numerical Evaluation of Strength in the Interface During Indentation Spherical Testing in Thin Films, *Mat. Sciences Applications*, 5, 149-157.
- [2] Fischer-Cripps, A.C., 2006, Critical Review of Analysis and Interpretation of Nanoindentation Test Data, *Surf. & Coatings Technology*, 200, 4153-4165.
- [3] Sun, Y., Bloyce A., Bell T., 1999, Finite Element Analysis of Plastic Deformation of Various TiN Coating/Substrate Systems under Normal Contact with a Rigid Sphere, *Thin Solid Films*, 271, 122-131.
- [4] Begley, M.R., Evans, A.G., Hutchinson, J.W., 1999, Spherical Impression of Thin Films on Elastic-plastic Substrates, *Int. Journal of Solids & structures*, 36, 2773-2788.
- [5] Zeng, K., Chiu, C-h., 2001, An Analysis of Load-Penetration Curves from Instrumented Indentation, *Acta Materialia*, 49, 3539-3551.
- [6] Lee, H., Lee, J.H., Pharr, G.M., 2005, A Numerical Approach to Spherical Indentation Techniques for Material Property Evaluation, *Journal of the Mechanics & Physics of Solids*, 53, 2073-2069.

- [7] Dias, A.M.S., Godoy, G.C.D., 2010, Determination of Stress-Strain Curve through Berkovich Indentation Testing, *Materials Science Forum*, 636-637, 1186-1193.
- [8] Pulécio, S.A.R., Farias, M.C.M., Souza, R.M., 2010, Finite element and dimensional analysis algorithm for the prediction of mechanical properties of bulk materials and thin films. *Surface & Coatings Technology*, 205(5), 1386-1392.
- [9] Mousse, C., Mauvoisin, G., Bartier, O., Pilvin, P., Delattre, G., 2012, Characterization of Homogenous and Plastically Graded Materials with Spherical Indentation and Inverse Analysis, *J. Materials Research*, 27 (1), 20-27.
- [10] Lichinchi, M., Lenardi, C., Haupt, J., Vitali, R., 1998, Simulation of Berkovich nanoindentation experiments on thin films using finite element method, *Thin Solid Films*, 333, 278-286.
- [11] Souza, R.M., Mustoe, G.G.W., Moore, J.J., 2001, Finite Element Modeling of the Stresses, Fracture and Delamination During the Indentation of Hard Elastic Films on Elastic-Plastic Soft Substrates, *Thin Solid Films*, 392, 65-74.
- [12] Bressan, J.D., Tramontin, A., Rosa, C., 2005, Modeling of nanoindentation of bulk and thin film by finite element method, *Wear*, 258, 115-122.
- [13] Dias, A.M.S., Modenesi, P.J., Godoy, G.C.D., 2006, Computer Simulation of Stress Distribution During Vickers Hardness Testing of WC-6Co, *Materials Research*, 9 (1), 73-76.
- [14] Fukumasu, N.K., Souza, R.M., 2015, Numerical evaluation of cohesive and adhesive failure modes during the indentation of coated systems with compliant substrates, *Surface & Coatings Technology*, 260, 266-271.
- [15] Libório, M.S., Dias, A.M.S., Souza, R.M., 2017, Determination of Film Thickness through Simulation of Vickers Hardness Testing, *Materials Research*, *submitted*.
- [16] Huang, X., Pelegri, A.A., 2005, Mechanical characterization of thin film materials with nanoindentation measurements and FE analysis, *Journal of Composite Materials*, 40, 1393-1407.
- [17] Dias, A.M.S., Sotani, P.F.B., Godoy, G.C., 2010, Simulação do Ensaio de Indentação em Filmes Finos com o Uso de Modelos de Trinca Difusa, *Revista Matéria*, 15 (3), 422-430. *In portuguese*.
- [18] Pulécio, S.A.R., Alcalá J., Souza, R.M., 2012, The reduced modulus in the analysis of sharp instrumented indentation tests, *Journal of Materials Research*, 27(16), 2148-2160.